

# Spontaneous and Partial Repair of Ribbon Synapse in Cochlear Inner Hair Cells After Ototoxic Withdrawal

Ke Liu · DaiShi Chen · WeiWei Guo · Ning Yu · XiaoYu Wang · Fei Ji · ZhaoHui Hou · Wei-Yan Yang · ShiMing Yang

Received: 1 September 2014 / Accepted: 20 October 2014 / Published online: 7 November 2014  
© Springer Science+Business Media New York 2014

**Abstract** Ototoxicity is one of the major causes of sensorineural deafness. However, it remains unclear whether sensorineural deafness is reversible after ototoxic withdrawal. Here, we report that the ribbon synapses between the inner hair cells (IHCs) and spiral ganglion nerve (SGN) fibers can be restored after ototoxic trauma. This corresponds with hearing restoration after ototoxic withdrawal. In this study, adult mice were injected daily with a low dose of gentamicin for 14 consecutive days. Immunostaining for RIBEYE/CtBP2 was used to estimate the number and size of synaptic ribbons in the cochlea. Hearing thresholds were assessed using auditory brainstem responses. Auditory temporal processing between IHCs and SGNs was evaluated by compound action potentials. We found automatic hearing restoration after ototoxicity withdrawal, which corresponded to the number and size recovery of synaptic ribbons, although both hearing and synaptic recovery were not complete. Thus, our study indicates that sensorineural deafness in mice can be reversible after ototoxic withdrawal due to an intrinsic repair of ribbon synapse in the cochlea.

**Keywords** Sensorineural deafness · Cochlea · Ribbon synapse · Ototoxic exposure · RIBEYE/CtBP2

## Introduction

Normal hearing requires successful sound signal encoding and conduction to the central nervous system (CNS). Previous

studies have reported that ototoxicity can cause sensorineural deafness in both animals and humans [1–5]. Ototoxicity tends to lead to morphologic changes in the cochlea, such as stereocilia disarray or loss, damaged hair cells, and spiral ganglion neurons (SGNs) degeneration, which result in hearing impairment [6–8]. We previously found that a moderate ototoxicity in mice could lead to a mild hearing loss without significant morphologic changes in the cochlea [9, 10]. This suggests that moderate ototoxicity may induce mild hearing loss via other mechanisms. Other study proposed that acoustic overexposure could induce changes of cochlear ribbon synapse, which may contribute to temporary hearing loss despite normal cochlear morphology [11]. Our previous study also proposed that cochlear ribbon synapse is a sensitive site to external insults [9, 10], leading to the hypothesis that changes of cochlear ribbon synapse may also be a key contributor to the hearing impairment induced by ototoxicity trauma.

Ribbon synapses in the cochlea locate between the hair cells and the terminals of primary auditory neurons (SGNs), and are considered the first afferent synaptic connection in the hearing pathway [12–14]. The ribbon synapses are characterized as having a pre-synaptic ribbon to which many synaptic vesicles are connected. The ribbon is anchored to the active zone of the ribbon synapse where exocytosis of the synaptic vesicle occurs [15–17]. The ribbon has been recognized as capable of a high rate of neurotransmitter release [18–20]. Most mammalian ribbon synapses develop as part of the sensory systems that require the highest rate of information transfer and sensory discrimination, such as vision and hearing. In this study, we aimed to study whether moderate aminoglycoside ototoxicity significantly disrupts ribbon synapse functioning in the cochlea of mice with only minor or no changes in hair cells and SGNs morphology. We also tried to determine whether synaptic changes, including ribbon synapse damage and repair, are consistent with

Ke Liu and Daishi Chen contributed equally to this work.

K. Liu · D. Chen · W. Guo · N. Yu · X. Wang · F. Ji · Z. Hou · W.-Y. Yang · S. Yang (✉)

Department of Otolaryngology-Head and Neck Surgery, the Institute of Otolaryngology, Chinese PLA General Hospital, 28 Fuxing Road, 100853 Beijing, China  
e-mail: Yangsm301@263.net

shifts of hearing thresholds in relation to ototoxicity. We found consistent hearing restoration and synapse repair in mice after ototoxicity withdrawal.

## Materials and Methods

### Animal Preparation and Procedure of Gentamicin Administration

Sixty female C57BL/6J mice (5 weeks of age) were obtained from the Chinese Academy of Medical Sciences Animal Center (Beijing, China). The mice (120 cochleae) were randomly divided into four groups (30 cochleae in each group): the control (0th day, no gentamicin treatment), 7th day, 14th day, and 28th day groups (after gentamicin treatment). All the mice were examined using an electrical otoscope to rule out outer or middle ear pathologies. For ototoxicity exposure, the mice were intraperitoneally injected with gentamicin sulfate (Invitrogen, CA) once a day at the dose of 100 mg/kg, and the treatment was successively performed for 14 days. The mice in the 7th day group were tested for hearing function and then sacrificed for morphological study on the 7th day of the gentamicin treatment. Similarly, the mice in the 14th day group were tested and sacrificed for morphological studies on the 14th day of the gentamicin treatment. The gentamicin treatment was ceased after the 14th day, and the mice in the 28th day group were kept gentamicin treatment-free for additional 14 days. In this study, all procedures were in accordance with the animal care and use protocols approved by the Animal Care and Use Committee of the PLA General Hospital.

### ABR Tests

Auditory brainstem response (ABR) thresholds of the mice were evaluated in a double blind manner. ABRs were measured with a smart-Epv2.21 from Intelligent Hearing Systems (Miami, FL, USA), which was used to generate specific acoustic stimuli and to amplify, measure, and display the evoked brainstem responses. The mice were anesthetized with 10 % chloral hydrate (0.0045 ml/g body weight) and kept warm with a heating pad. Testing was done in a soundproof shielded room. For ABR recordings, subdermal needle electrodes were inserted at the vertex and locations ventrolateral to the ear. Specific auditory stimuli (broadband clicks and tone pips of 1, 2, 4, 8, and 16 kHz), with 20 beats/s recurrence rate, were delivered through plastic tubes in the ear canals to left and right ear, respectively. ABR signals were amplified with a filtering bandwidth of 100 Hz–3 kHz and 1,024 samples were acquired and averaged for each stimulus intensity.

### Compound Action Potentials (CAPs) Recording

Click-evoked CAPs were produced using a commercially available TDT system II by delivering 80  $\mu$ s rectangular pulses to a speaker (MF1, TDT), placed 10 cm in front of the animal's ears. The phase of every other click signals was alternated so that the cochlear microphonics were canceled out. Click signal levels ranged from 90 to 0 dB SPL, decreasing in 10 dB steps and were presented at a rate of 11.1 s. To record CAPs, a silver ball electrode was placed on the round window membrane via an opening in the mastoid. The electrode was secured in place with dental cement. The reference and grounding electrodes were subdermal needles inserted behind the ears.

### Cochlear Tissue Processing

After ABR recordings, the mice were sacrificed by cervical dislocation and decapitation. The temporal bone was removed, and the cochlea was quickly separated. The round and oval windows were opened and perfused with 4 % paraformaldehyde and left in a 10 % EDTA solution at 4 °C overnight. The cochlea shell was separated from the basal turn under a dissecting microscope in 0.01 mmol/l PBS solution. The apical turn basilar membrane was separated, and the vestibular membrane and tectorial membrane were removed. The cochlear specimens were processed for light microscopy using the standard method including embedding in celloidin, serial sectioning in the horizontal plane at a section thickness of 20  $\mu$ m, and staining of every tenth section using hematoxylin and eosin (HE staining).

### Immunostaining

Specimens were fixed in 4 % paraformaldehyde and dissolved in 0.1 M PBS with 30 % sucrose (pH 7.4) for 1 h at room temperature. They were washed three times in 0.01 M PBS and pre-incubated for 30 min at room temperature in blocking solution of 5 % normal goat serum in 0.01 M PBS with 0.3 % Triton X-100. Next, specimens were incubated with anti-CtBP2 (1:200, Ca<sup>#</sup>: 612044, BD) at 4 °C overnight. After incubation, the specimens were washed in 0.01 M PBS three times and incubated with the secondary antibody IgG FITC identifying anti-CtBP2 (1:200, Ca<sup>#</sup>: 1296479, Invitrogen) at 37 °C for 40 min. After incubation, the specimens were washed in PBS twice. Approximately 40  $\mu$ l of DAPI (4', 6-diamidino-2-phenylindole; Santa Cruz) was applied to the slide. The basilar membrane was mounted under a dissecting microscope. The specimens were imaged directly with fluorescent microscopy to examine the specificity of the primary antibody. Controls were performed to demonstrate negative staining (data not shown).

## Confocal Microscopy Imaging

For confocal microscopy imaging, laser scanning confocal microscopy was conducted using a Leica TCS SP2 AOBs (Germany) with a  $\times 100$  oil immersion objective lens. Excitation wavelengths were 488 and 568 nm, and local images were digitally magnified by twofold. Sequence scanning was performed at an interval of 1.0  $\mu\text{m}$ . All digital images were captured under identical exposure and light settings. Images were processed into a virtual file format, transferred to the Definiens share, and a Definiens zoom cache was created. Virtual slides were then uploaded and rule sets were developed using the Definiens software.

## Electron Microscopy

For the scanning electron microscopy (SEM) examination, mice were sacrificed and the cochleae were removed. All cochleae were pre-fixed in 2.5 % glutaraldehyde and then placed in 1 % OsO<sub>4</sub> in 0.1 M PBS (pH 7.40) for 2 h at room temperature. After a thorough rinse with 0.1 M PBS, the specimens were dissected in 0.1 M PBS to expose the organs of Corti. After dehydration in a graded series of alcohol, specimens were dried in an HCP-2 critical point dryer and sputter-coated with platinum for 4 min in an E-102 ion sputter. The samples were then examined under a JEOL JSM-35C scanning electron microscope (Hitachi 7100, Japan). The images were recorded digitally and photographed.

## Statistical Analysis

All data are presented as mean  $\pm$  SD. Data were examined using a one-way ANOVA with Student-Newman-Keuls test or Dunnett's multiple comparison post-test statistical analysis to determine the differences between groups. Variegated synaptic ribbon was defined as those falling outside 2 standard deviations of the normal mean ( $0.57 \pm 0.2 \mu\text{m}$ ) for synaptic ribbon size. All statistical analyses were performed using the SPSS16.0 statistical software package. A *p* value  $<0.05$  was considered statistically significant.

## Results

### Automatic Hearing Restoration After Ototoxicity Withdrawal

We used ABRs to measure ototoxicity-induced hearing threshold shifts. Mean ABR thresholds among the control mice were  $40.14 \pm 5.69$ ,  $40.05 \pm 6.56$ ,  $43.57 \pm 7.79$ ,  $41.05 \pm 4.31$ ,  $33.75 \pm 4.33$ , and  $29.21 \pm 3.14$  dB SPL for clicks and tone pips at 1, 2, 4, 8, and 16 kHz, respectively (Fig. 1). Maximal hearing loss was observed after 7 days of ototoxicity

exposure at  $54.12 \pm 7.25$ ,  $63.18 \pm 9.15$ ,  $61.29 \pm 8.13$ ,  $53.10 \pm 4.82$ ,  $47.58 \pm 5.73$ , and  $45.54 \pm 5.36$  dB SPL for clicks and tone pips at 1, 2, 4, 8, and 16 kHz, respectively, significantly higher than those of the control mice (*p* < 0.01, Fig. 1). The mean ABR thresholds after 14 days of ototoxicity exposure were  $50.33 \pm 5.24$ ,  $54.72 \pm 6.37$ ,  $55.17 \pm 7.31$ ,  $50.65 \pm 5.39$ ,  $42.76 \pm 6.84$ , and  $38.79 \pm 7.08$  dB SPL for clicks and tone pips at 1, 2, 4, 8, and 16 kHz, respectively, showing no statistically significant difference from those 7 days after ototoxicity exposure (*p* > 0.05). Continued ototoxic exposure did not seem to cause further hearing thresholds increase between the 7th and 14th days of exposure. In this study, ototoxicity exposure was terminated after 14 days. The mean ABR thresholds obtained on day 28 were  $44.37 \pm 4.12$ ,  $47.10 \pm 5.22$ ,  $49.58 \pm 5.43$ ,  $43.23 \pm 3.45$ ,  $36.35 \pm 3.03$ , and  $33.37 \pm 2.95$  dB SPL for clicks and tone pips at 1, 2, 4, 8, and 16 kHz, respectively, significantly lower than those after 7 and 14 days of ototoxicity exposure (*p* < 0.01, Fig. 1), although still significantly higher than those of the control mice (*p* < 0.01, Fig. 1). Hearing appeared to have spontaneously restored after ototoxicity withdrawal, although this recovery was incomplete.

### Synaptic Ribbons Number Restoration After Ototoxic Withdrawal

The number of ribbons was determined via immunostaining for RIBEYE/CtBP2 [21–23]. The majority of synaptic ribbons were located inside the cochlear IHCs (Fig. 2a, green spots in the right panel). Adjacent optical sections of the basal, middle, and apical turns were used to count the number of ribbons (Fig. 2a, left and right panels). The mean number of synaptic ribbons per IHC (from 105 IHCs of 16 cochleae) in the control mice was  $14.70 \pm 1.56$  in the basal turn,  $12.47 \pm 1.28$  in the middle turn, and  $9.31 \pm 0.72$  in the apical turn (Fig. 2b, the panel of control; Fig. 2c, the white columns). The mean number of ribbons per IHC (from 123 IHCs of 18 cochleae) in mice after 7 days of ototoxicity exposure was  $9.35 \pm 1.17$  in the basal turn,  $9.03 \pm 0.94$  in the middle turn, and  $7.25 \pm 0.62$  in the apical turn (Fig. 2b, the panel of 7th d; Fig. 2c, the light gray columns), significantly lower than those seen in the control mice (*p* < 0.01, Fig. 2c). The ototoxic seemed to reduce the number of synaptic ribbons in the cochlea.

Next, we analyzed the number of ribbons after 14 days of ototoxicity exposure. The mean number of ribbon per IHC (from 112 IHCs of 16 cochleae) was  $5.41 \pm 0.72$  in the basal turn,  $5.05 \pm 0.60$  in the middle turn, and  $4.54 \pm 0.66$  in the apical turn (*p* < 0.01, Fig. 2b, the panel of 14th d; Fig. 2c, the dark gray columns), showing continued decrease under continuous ototoxicity exposure. On day 28 (14 days after ototoxic withdrawal), the mean number of synaptic ribbons was  $12.17 \pm 1.20$  in the basal turn,  $10.73 \pm 0.97$  in the middle turn, and  $7.98 \pm 0.66$  in the apical turn (Fig. 2b, the panel of 28th d;

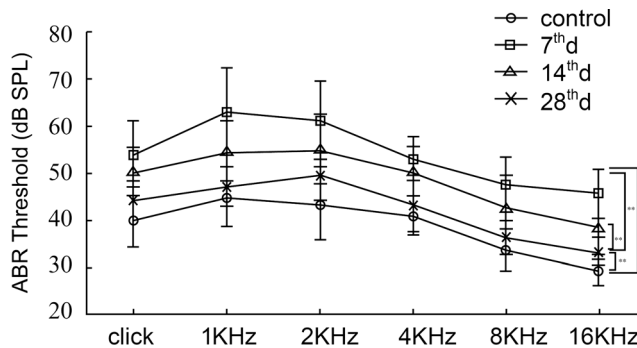


**Fig. 1** Spontaneous hearing restoration after ototoxic withdrawal. The mean ABR thresholds in response to clicks and tone pips at 1, 2, 4, 8, and 16 kHz for the control group and on the 7th and 14th days of ototoxicity, and on day 28 (14 days after ototoxic withdrawal) are shown. ABR thresholds are significantly higher 7 days after ototoxicity exposure ( $p<0.01$ , double asterisk) compared to the controls but are not significantly different between days 14 and 7 of ototoxicity exposure ( $p>0.05$ , no asterisk). ABR thresholds are significantly lower on day 28 compared to days 7 and 14 of ototoxicity exposure ( $p<0.01$ , double asterisk), although still higher than the controls ( $p<0.01$ , double asterisk)

Fig. 2c, the black columns), significantly higher than the mean numbers of ribbons after 7 and 14 days of ototoxicity exposure ( $p<0.01$ , but still significantly lower than those in the control mice  $p<0.01$ ). The number of cochlear synaptic ribbons seemed to be restored after ototoxic withdrawal, although the restoration was again incomplete.

#### Restoration of Size of Synaptic Ribbon After Ototoxic Withdrawal

Variegated ribbon synapse sizes may reflect sensory synaptic plasticity in individual synapses [24–26]. In this study, the size of each ribbon was estimated using the immunostained spot collected and measured using the Image-Pro Plus software (Fig. 3a). We found normal distribution of the size of synaptic ribbons in the control group at  $0.57\pm 0.2$   $\mu\text{m}$  (Fig. 3b). As described in the “Statistical Analysis” section of “Materials and Methods,” any immunostained spot exceeding  $0.57\pm 2 \times 0.2$   $\mu\text{m}$  would be defined as a variegated ribbon because spots of a size less than  $0.57\pm 2 \times 0.2$   $\mu\text{m}$  were near the background of immunostaining particles (anti-CtBP2). For this reason, in this study, there were very few variegated synapses identified in the control mice:  $0.41\pm 0.08$  in the basal turn,  $0.34\pm 0.07$  in the middle turn, and  $0.27\pm 0.08$  in the apical turn (Fig. 3b, the white columns). The number of variegated synaptic ribbons significantly increased after ototoxic trauma ( $p<0.01$ ). The maximal number of variegated ribbons was  $4.24\pm 0.38$  in the basal turn,  $3.42\pm 0.32$  in the middle turn, and  $2.98\pm 0.22$  in the apical turn and occurred after 7 days of ototoxicity exposure (Fig. 3b, the light gray columns). The mean number of variegated synaptic ribbons after 14 days of ototoxicity exposure was  $3.02\pm 0.25$  in the basal turn,  $3.13\pm 0.28$  in the middle turn, and  $2.36\pm 0.17$  in the apical turn (Fig. 3b, the dark gray

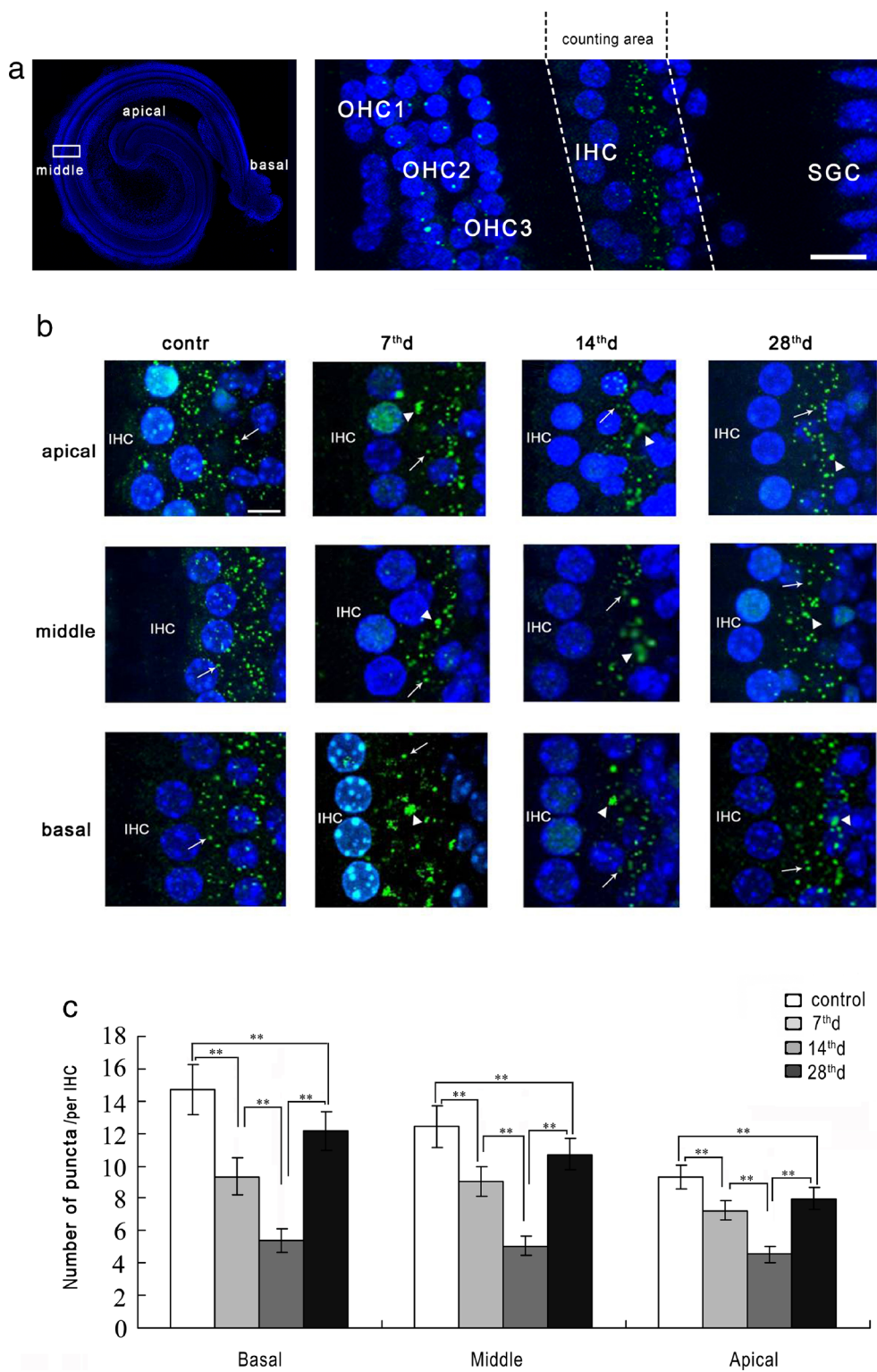
**Fig. 2** Restoration of number of synaptic ribbons after ototoxic withdrawal. **a** A representative sample from the middle turn of the cochlea (left panel) with each RIBEYE/CtBP2 punctum representing a synaptic ribbon. All immunostained synaptic ribbons are seen below the nuclei of IHCs (right panel, green) and between the IHCs and spiral ganglion cells (SGCs). IHC nuclei are stained using DAPI (blue). Scale bar=10  $\mu\text{m}$ . **b** Changes in the number and size of synaptic ribbons in response to continuous ototoxicity exposure. Synaptic ribbons are marked by RIBEYE/CtBP2 immunostaining. Large number of ribbon synapses (arrows) are present in the basal, middle, and apical turns of the cochlea in control mice (panel of the control). The number and size of synaptic ribbons are affected after 7 and 14 days of ototoxicity (panels of 7th and 14th day, arrows indicate synaptic ribbons and arrowheads indicate variegated synaptic ribbons) but shows recovery on day 28 (panel of 28th day). Scale bar=5  $\mu\text{m}$ . **c** Number of synaptic ribbons per inner hair cell (IHC) before and after ototoxic withdrawal. The number of synaptic ribbons is significantly lower after 7 days of ototoxicity exposure as compared to the controls but higher than after 14 days after exposure and on day 28 ( $p<0.01$ ). The number on day 28 is higher than after 7 and 14 days of ototoxicity after exposure ( $p<0.01$ ), although still lower than the controls ( $p<0.01$ )

columns). On the 28th day, the mean number of variegated ribbons in the basal, middle, and apical turns showed significant decrease compared with those on the 7th and 14th days of exposure ( $p<0.01$ ), although still higher than those of the control ( $p<0.01$ , Fig. 3b, the black columns).

Next, we compared the number alterations of synaptic ribbons across frequencies in the cochlea during the ototoxic exposure. We found that the number of ribbons in the basal turn was significantly higher than those in the middle and apical turns (Fig. 4a). Similarly, the number of variegated ribbons across frequencies in the cochlea showed significantly more variability in the basal turn than those in the middle and apical turns (Fig. 4b). The ribbon synapses formed at or near the basal turn of the cochlea appeared to be more susceptible to ototoxicity exposure compared with those in the middle and apical turns.

#### Restoration of CAPs After Ototoxic Withdrawal

We also measured CAPs to estimate possible synaptic damage and repair at the IHC-SGN synaptic connection. The mean CAP threshold was  $37.20\pm 5.60$  dB SPL in the control mice,  $52.50\pm 6.81$  dB SPL after 7 days of exposure,  $48.35\pm 5.50$  dB SPL after 14 days of exposure, and  $41.50\pm 4.28$  dB SPL on day 28 (Fig. 5). Maximal CAP threshold elevation was observed after 7 days of exposure, to some degree reflecting disturbed IHC-SGN synaptic connection by the ototoxic exposure. CAP thresholds were significantly lower on day 28 (14 days after ototoxic withdrawal) than after 7 days of ototoxicity exposure ( $p<0.01$ ), although still significantly higher than the control mice ( $p<0.05$ , Fig. 5). These results may suggest that the function of ribbon synapses is partially repaired after ototoxic withdrawal.



#### Absence of Significant Disruption in OHCs and SGCs Morphology

SEM was used to examine whether cochlear components, such as the stereocilia and auditory nerve fibers, were

significantly affected by the ototoxic exposure. Despite significant alterations of synaptic ribbons, no significant disruption in OHCs or spiral ganglion cells (SGCs) were found (Fig. 6). The stereocilia of OHCs also showed normal appearance in all groups (Fig. 6a, c, e, g). Similarly, there were no

significant differences in both the density and innervations of SGNs across all groups (Fig. 6b, d, f, h).

## Discussion

Ototoxicity has been considered a primary contributor to irreversible hearing loss [3, 27]. The underlying mechanism behind ototoxicity-induced hearing loss is currently thought to be the permanent loss of hair cells or SGNs in the cochlea [8, 18]. In this study, we showed that hearing loss induced by moderate ototoxicity was reversible after ototoxic withdrawal. Moreover, this reversible hearing loss did not lead to the loss or degeneration of cochlear components, such as the stereocilia and auditory nerves. Our investigation also showed that the hearing restoration might be due to the repair of ribbon synapses in the cochlea.

Normal mammalian hearing function depends primarily on synaptic release at ribbon synapses [28–30]. For example, otoferlin is thought to play a key role in exocytosis at IHC ribbon synapses [31]. Gentamicin ototoxicity has been

reported to interrupt otoferlin expression in IHCs, subsequently resulting in hearing disorders in mice [9]. This suggests that IHC ribbon synapses may have been disturbed by gentamicin ototoxicity. In this study, we further demonstrated that ototoxicity-induced hearing loss corresponded with number and size changes of synaptic ribbons in the cochlea in mice. Furthermore, restoration of hearing was consistent with changes of synaptic ribbons after ototoxic withdrawal. Thus, our findings appear to provide direct evidence that synaptic repair may serve as the underlying mechanism for the deafness from ototoxicity and hearing restoration after ototoxic withdrawal.

We note that our findings may not be consistent with some other previous studies [8, 18] that proposed that the permanent loss of hair cells or SGNs is the primary cause of hearing loss. One possible explanation for the conflicting results is that those studies have been conducted *in vitro* where ototoxic substrates were directly applied to the hair cells or auditory nerves, leading to severely damaged hair cells or auditory nerves. In our study, mice were subjected to exposure of gentamicin which might not easily bypass the labyrinthine barrier in the cochlea to directly affect cochlear components.

**Fig. 3** Restoration of number of variegated synaptic ribbons after ototoxic withdrawal. **a** Both synaptic ribbons and nuclei of inner hair cells are labeled by antibodies against RIBEYE/CtBP2 (green), scale bar=20  $\mu$ m. The size of spots identified by RIBEYE/CtBP2 is measured using the Image-Pro Plus software (white frames). Panels on right show amplified frames in the left panel. Variegated synaptic ribbons are defined as exceeding 2 standard deviations of the normal mean ( $0.57 \pm 0.2 \mu\text{m}$ ). **b** The highest number of variegated synaptic ribbons is on day 7 of ototoxicity exposure, significantly higher than the control ( $p < 0.01$ ) and then day 14 of ototoxic exposure ( $p < 0.01$ ). The number on day 28 shows a significant decrease significantly in comparison to on the 7th and 14th days of exposure ( $p < 0.01$ ), although still higher than the control ( $p < 0.01$ )

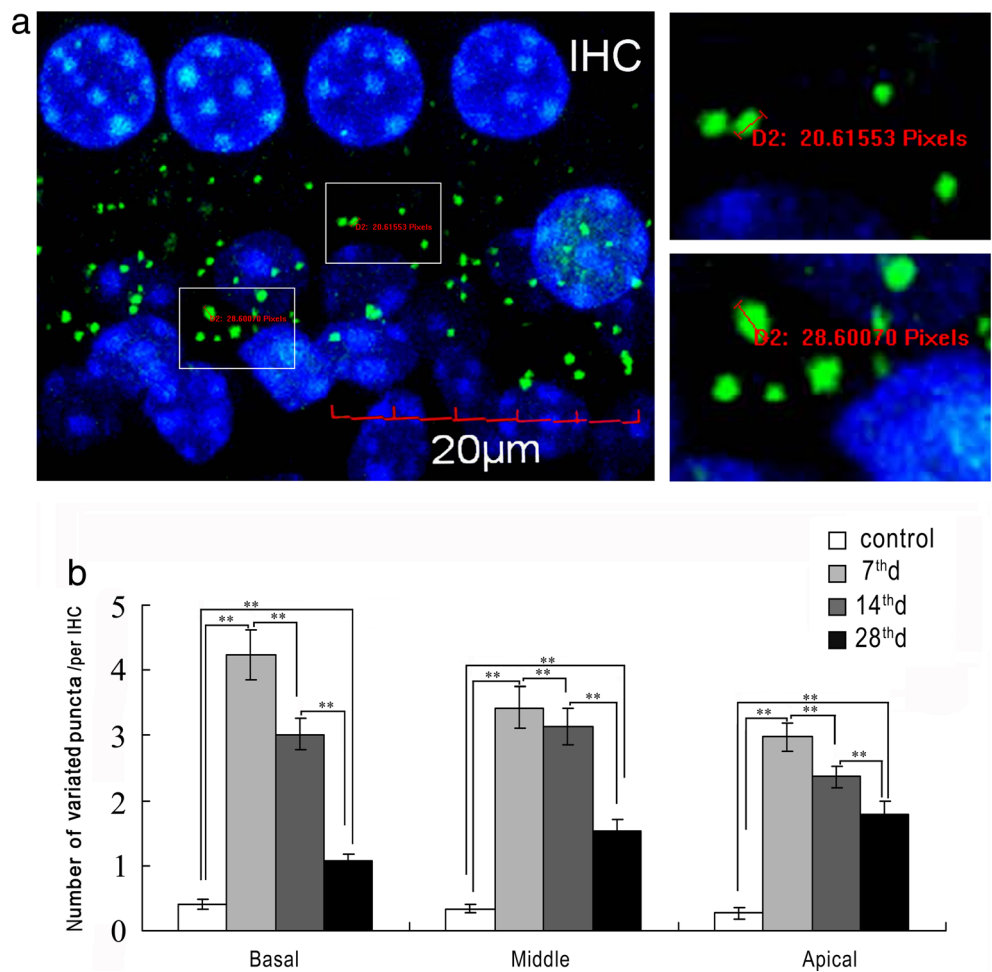
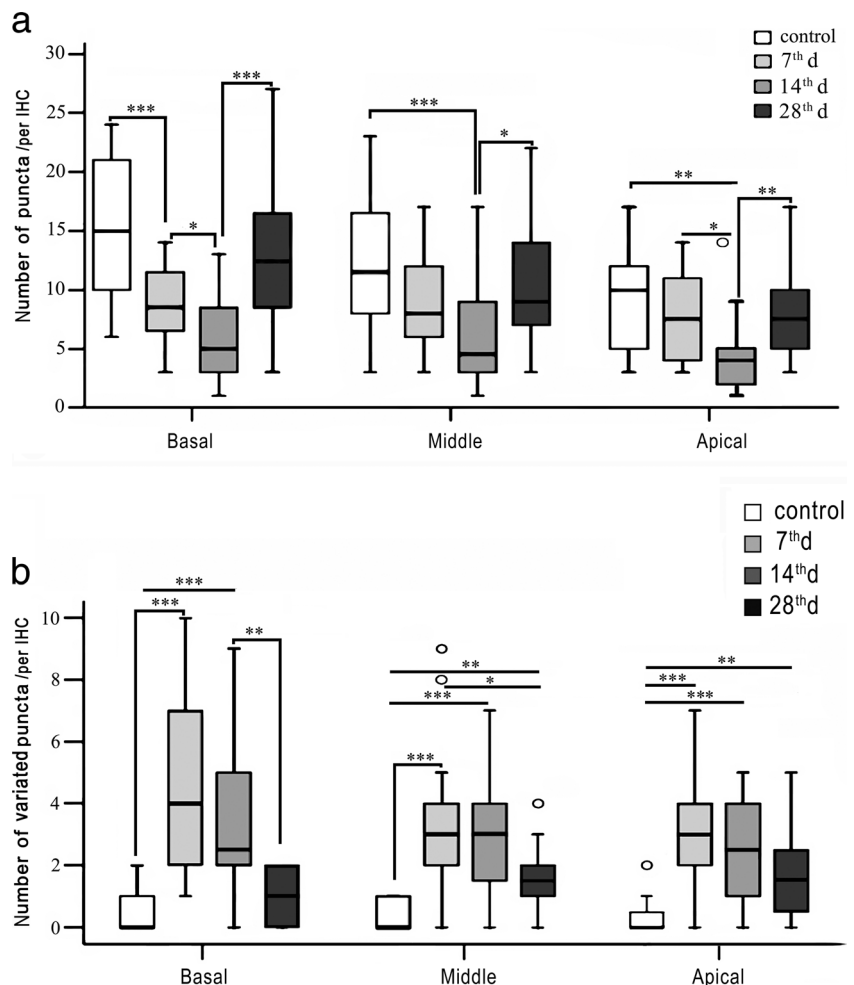


**Fig. 4** Frequency-specific alterations of synaptic ribbons after ototoxicity exposure. **a** Ototoxicity exposure affects the number of synaptic ribbon synapses in the basal turn of the cochlea more than in the middle and apical turns. **b** Ototoxicity exposure induces more size changes of synaptic ribbons in the basal turn of cochlea than in the middle and apical turns



Supporting data can be found in another study, where application of large dosage kanamycin was unable to induce hair cell loss until 2 weeks after exposure [32].

RIBEYE was first identified as a major component of cochlear ribbon synapses using synaptic ribbon-enriched bovine retinal extract [33]. RIBEYE is specific to ribbon synapse

and is thought to help assemble other proteins into the ribbon and drive ribbons to pre-synaptic fusion sites [28, 30, 34, 35]. RIBEYE is comprised of two domains and domain B contains a partial C-terminal binding protein 2 (CtBP2) sequence [36]. The size, shape, and number of synaptic ribbons are generally thought to significantly impact synaptic signaling [17, 23, 37–40].

In this study, we identified ribbon synapses by immunostaining for RIBEYE/CtBP2 puncta. We found that the number of synaptic ribbons significantly decreased after 7 and 14 days of ototoxicity exposure, which corresponded with elevated hearing thresholds. Furthermore, the number of ribbon synapses increased on day 28 (14 days after ototoxic withdrawal), which also corresponded with hearing improvement. The size of the ribbon was also significantly affected by ototoxicity. Variegated synaptic ribbons were larger in mice exposed to the ototoxic agent and decreased in size after ototoxic withdrawal. These changes were consistent with ABR threshold shifts. Our data indicate that variations in ribbon size can, in part, reflect hearing function. These data are supported by a previous study which suggested that synaptic ribbons and postsynaptic density may reflect hearing

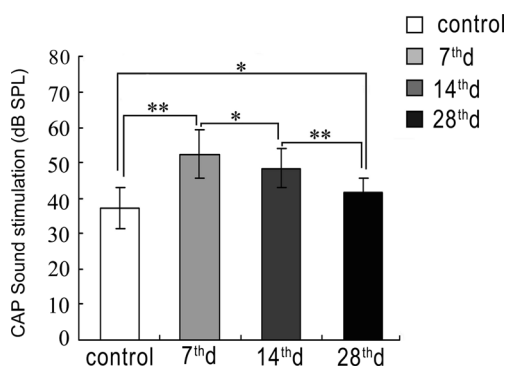
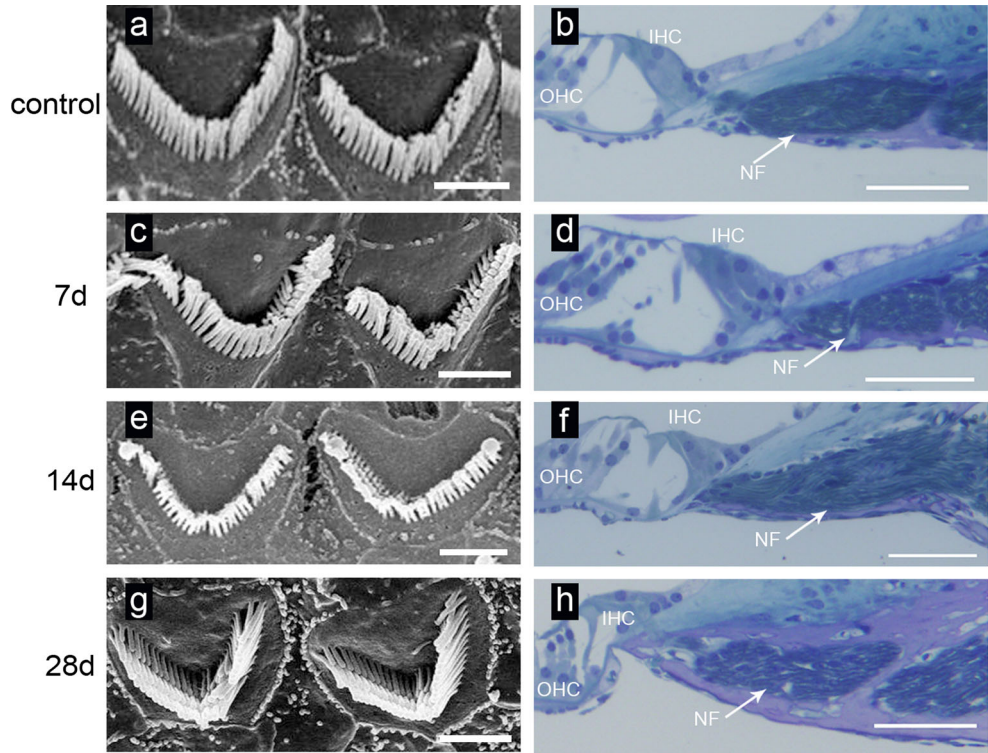


**Fig. 5** Restoration of CAPs after ototoxic withdrawal. CAP thresholds are higher after 7 days of ototoxicity exposure than the controls ( $p<0.01$ , double asterisk) but has become lower on day 28 ( $p<0.01$ , double asterisk), although still higher than the controls ( $p<0.05$ , asterisk). The highest CAP threshold is observed after 7 days of ototoxicity

**Fig. 6** No significant change in morphology of hair cells and auditory nerves from ototoxicity exposure. Scanning electron microscopy (SEM) shows no significant changes in the stereocilia of OHCs before and after ototoxicity (a, c, e, g). Scale bar=20  $\mu$ m. Semi-thin sections of OHCs, IHCs, and auditory nerves show no significant differences before and after ototoxic withdrawal. There are three well-organized rows of OHCs, one row of IHCs, and regular density of spiral ganglion cells (SGCs) nerve fibres (NF, white arrows) in all groups (b, d, f, h). Scale bar=50  $\mu$ m



function [41]. In that study, noise trauma induced transient changes in the size of ribbon synapses, and ribbon synapses recovered within 1 month after the noise exposure [41]. We also found different distributions of variegated synaptic ribbons along cochlear turns. Ribbon synapses formed at or near the basal turn of the cochlea appeared to be more susceptible to the ototoxic exposure. Correspondingly, previous studies have proposed that hair cells in the basal turn of the cochlea are also more susceptible to ototoxic stimuli than those in the middle and apical turns [1, 42–44].

We previously showed that IHC ribbon synapses were the primary target of aminoglycoside ototoxicity [10]. Other studies have shown that noise overexposure can also cause “silent damage” to ribbon synapses despite intact hair cells and SGNs [11, 45]. We have also found that IHC ribbon synapse-associated proteins, such as RIBEYE or otoferlin, are significantly affected by gentamycin ototoxicity [9, 10, 45]. Similarly, aminoglycosides have been proposed to inhibit protein synthesis by facilitating the erroneous pairing of non-agnate tRNAs, thereby increasing the error rate of translation [1, 5]. Additional evidence from cultured aplysia sensory synapses shows that local protein synthesis at or near the synapses is significantly inhibited by anisomycin [24, 26].

It is generally agreed that CAPs are generated by electrical activities at the terminal of SGN fibers [46]. Thus, CAP has been considered a functional indicator of afferent synaptic activities of SGN fibers [46–48]. In this study, we further explored the effects of ototoxicity on the

temporal processing capability of the auditory system. We evaluated cochlear responses by measuring CAPs to time-stress signals compared with the loss and repair of synaptic ribbons. We showed that CAPs changes correlated with hearing loss and changes in the number and size of synaptic ribbons in the cochlea. In addition, we found that ototoxic exposure did not significantly change the morphology of hair cells and SGNs. Therefore, our results in this study, together with those of our previous studies [9, 10, 45], may indicate that hearing loss can be reversed as long as hair cells and SGNs are intact. However, the hearing loss may no longer be reversible if ototoxicity exposure has caused significant loss of hair cells or SGNs [7, 8, 18].

In summary, we found that spontaneous hearing restoration following ototoxicity exposure in mice corresponded with the repair of cochlear synaptic ribbons. This suggests that spontaneous repair of ribbon synapse may serve as the molecular mechanism for hearing restoration. However, further investigations are required to determine how ribbon synaptic function changes in response to ototoxicity stimuli with no apparent morphological alterations.

**Acknowledgments** This work was supported by grants from the National Basic Research Program of China (973Program) (2012CB967900; 2012CB967901) and Beijing Natural Science Foundation (5122040). Additionally, this work was supported by grants from the China Postdoctoral Science Foundation (201003779; 20100470103) and the National Natural Science Foundation of China (NSFC) (31040038).

## References

- Komune S, Ide M, Nakano T, Morimitsu T (1987) Effects of kanamycin sulfate on cochlear potentials and potassium ion permeability through the cochlear partitions. *ORL J Otorhinolaryngol Relat Spec* 49(1):9–16
- Nakagawa T, Yamane H, Shibata S, Nakai Y (1997) Gentamicin ototoxicity induced apoptosis of the vestibular hair cells of guinea pigs. *Eur Arch Otorhinolaryngol* 254(1):9–14
- Wu WJ, Sha SH, McLaren JD, Kawamoto K, Raphael Y, Schacht J (2001) Aminoglycoside ototoxicity in adult CBA, C57BL and BALB mice and the Sprague-Dawley rat. *Hear Res* 158(1–2):165–178
- Gooi A, Hochman J, Wellman M, Blakley L, Blakley BW (2008) Ototoxic effects of single-dose versus 19-day daily-dose gentamicin. *J Otolaryngol Head Neck Surg* 37(5):664–667
- Perletti G, Vral A, Patrosso MC, Marras E, Ceriani I, Willems P, Fasano M, Magri V (2008) Prevention and modulation of aminoglycoside ototoxicity (review). *Mol Med Rep* 1(1):3–13
- Webster M, Webster DB (1981) Spiral ganglion neuron loss following organ of Corti loss: a quantitative study. *Brain Res* 212(1):17–30
- McFadden SL, Ding D, Jiang H, Salvi RJ (2004) Time course of efferent fiber and spiral ganglion cell degeneration following complete hair cell loss in the chinchilla. *Brain Res* 997(1):40–51
- Ding D, Jiang H, Salvi RJ (2010) Mechanisms of rapid sensory hair-cell death following co-administration of gentamicin and ethacrynic acid. *Hear Res* 259(1–2):16–23. doi:10.1016/j.heares.2009.08.008
- ShuNa L, Zhong R, Ke L (2009) A pattern of otoferlin expression interrupted by gentamicin exposure in ribbon synapse of inner hair cell in C57BL/6J mice. *Acta Neurol Belg* 109(3):221–225
- Liu K, Jiang X, Shi C, Shi L, Yang B, Shi L, Xu Y, Yang W, Yang S (2013) Cochlear inner hair cell ribbon synapse is the primary target of ototoxic aminoglycoside stimuli. *Mol Neurobiol* 48(3):647–654. doi:10.1007/s12035-013-8454-2
- Kujawa SG, Liberman MC (2009) Adding insult to injury: cochlear nerve degeneration after “temporary” noise-induced hearing loss. *J Neurosci* 29(45):14077–14085. doi:10.1523/JNEUROSCI.2845-09.2009
- Sidi S, Busch-Nentwich E, Friedrich R, Schoenberger U, Nicolson T (2004) Gemini encodes a zebrafish L-type calcium channel that localizes at sensory hair cell ribbon synapses. *J Neurosci* 24(17):4213–4223. doi:10.1523/JNEUROSCI.0223-04.2004
- Moser T, Neef A, Khimich D (2006) Mechanisms underlying the temporal precision of sound coding at the inner hair cell ribbon synapse. *J Physiol* 576(Pt 1):55–62. doi:10.1113/jphysiol.2006.114835
- Stamataki S, Francis HW, Lehar M, May BJ, Ryugo DK (2006) Synaptic alterations at inner hair cells precede spiral ganglion cell loss in aging C57BL/6J mice. *Hear Res* 221(1–2):104–118. doi:10.1016/j.heares.2006.07.014
- Lenzi D, Crum J, Ellisman MH, Roberts WM (2002) Depolarization redistributes synaptic membrane and creates a gradient of vesicles on the synaptic body at a ribbon synapse. *Neuron* 36(4):649–659
- Keen EC, Hudspeth AJ (2006) Transfer characteristics of the hair cell's afferent synapse. *Proc Natl Acad Sci U S A* 103(14):5537–5542. doi:10.1073/pnas.0601103103
- Johnson SL, Forge A, Knipper M, Munkner S, Marcotti W (2008) Tonotopic variation in the calcium dependence of neurotransmitter release and vesicle pool replenishment at mammalian auditory ribbon synapses. *J Neurosci* 28(30):7670–7678. doi:10.1523/JNEUROSCI.0785-08.2008
- Ding D, Stracher A, Salvi RJ (2002) Leupeptin protects cochlear and vestibular hair cells from gentamicin ototoxicity. *Hear Res* 164(1–2):115–126
- Glowatzki E, Fuchs PA (2002) Transmitter release at the hair cell ribbon synapse. *Nat Neurosci* 5(2):147–154. doi:10.1038/nn796
- Griesinger CB, Richards CD, Ashmore JF (2005) Fast vesicle replenishment allows indefatigable signalling at the first auditory synapse. *Nature* 435(7039):212–215. doi:10.1038/nature03567
- Khimich D, Nouvian R, Pujol R, Tom Dieck S, Egner A, Gundelfinger ED, Moser T (2005) Hair cell synaptic ribbons are essential for synchronous auditory signalling. *Nature* 434(7035):889–894. doi:10.1038/nature03418
- Nemzou NR, Bulankina AV, Khimich D, Giese A, Moser T (2006) Synaptic organization in cochlear inner hair cells deficient for the CaV1.3 (alpha1D) subunit of L-type  $\text{Ca}^{2+}$  channels. *Neuroscience* 141(4):1849–1860. doi:10.1016/j.neuroscience.2006.05.057
- Meyer AC, Frank T, Khimich D, Hoch G, Riedel D, Chapochnikov NM, Yarin YM, Harke B, Hell SW, Egner A, Moser T (2009) Tuning of synapse number, structure and function in the cochlea. *Nat Neurosci* 12(4):444–453. doi:10.1038/nn.2293
- Liu K, Hu JY, Wang D, Schacher S (2003) Protein synthesis at synapse versus cell body: enhanced but transient expression of long-term facilitation at isolated synapses. *J Neurobiol* 56(3):275–286. doi:10.1002/neu.10242
- Hu JY, Glickman L, Wu F, Schacher S (2004) Serotonin regulates the secretion and autocrine action of a neuropeptide to activate MAPK required for long-term facilitation in *Aplysia*. *Neuron* 43(3):373–385. doi:10.1016/j.neuron.2004.07.011
- Hu JY, Baussi O, Levine A, Chen Y, Schacher S (2011) Persistent long-term synaptic plasticity requires activation of a new signaling pathway by additional stimuli. *J Neurosci* 31(24):8841–8850. doi:10.1523/JNEUROSCI.1358-11.2011
- Abrashkin KA, Izumikawa M, Miyazawa T, Wang CH, Crumling MA, Swiderski DL, Beyer LA, Gong TW, Raphael Y (2006) The fate of outer hair cells after acoustic or ototoxic insults. *Hear Res* 218(1–2):20–29. doi:10.1016/j.heares.2006.04.001
- Nouvian R, Beutner D, Parsons TD, Moser T (2006) Structure and function of the hair cell ribbon synapse. *J Membr Biol* 209(2–3):153–165. doi:10.1007/s00232-005-0854-4
- Neef A, Khimich D, Pirih P, Riedel D, Wolf F, Moser T (2007) Probing the mechanism of exocytosis at the hair cell ribbon synapse. *J Neurosci* 27(47):12933–12944. doi:10.1523/JNEUROSCI.1996-07.2007
- Zanazzi G, Matthews G (2009) The molecular architecture of ribbon presynaptic terminals. *Mol Neurobiol* 39(2):130–148. doi:10.1007/s12035-009-8058-z
- Roux I, Safieddine S, Nouvian R, Grati M, Simmler MC, Bahloul A, Perfettini I, Le Gall M, Rostaing P, Hamard G, Triller A, Avan P, Moser T, Petit C (2006) Otoferlin, defective in a human deafness form, is essential for exocytosis at the auditory ribbon synapse. *Cell* 127(2):277–289. doi:10.1016/j.cell.2006.08.040
- Yu L, Jiang XH, Zhou Z, Tsang LL, Yu MK, Chung YW, Zhang XH, Wang AM, Tang H, Chan HC (2011) A protective mechanism against antibiotic-induced ototoxicity: role of prestin. *PLoS ONE* 6(2):e17322. doi:10.1371/journal.pone.0017322
- Schmitz F, Konigstorfer A, Sudhof TC (2000) RIBEYE, a component of synaptic ribbons: a protein's journey through evolution provides insight into synaptic ribbon function. *Neuron* 28(3):857–872
- Wan L, Almers W, Chen W (2005) Two ribeye genes in teleosts: the role of Ribeye in ribbon formation and bipolar cell development. *J Neurosci* 25(4):941–949. doi:10.1523/JNEUROSCI.4657-04.2005
- Magupalli VG, Schwarz K, Alpadi K, Natarajan S, Seigel GM, Schmitz F (2008) Multiple RIBEYE-RIBEYE interactions create a dynamic scaffold for the formation of synaptic ribbons. *J Neurosci* 28(32):7954–7967. doi:10.1523/JNEUROSCI.1964-08.2008
- Moser T, Brandt A, Lysakowski A (2006) Hair cell ribbon synapses. *Cell Tissue Res* 326(2):347–359. doi:10.1007/s00441-006-0276-3
- Hull C, Studholme K, Yazulla S, von Gersdorff H (2006) Diurnal changes in exocytosis and the number of synaptic ribbons at active zones of an ON-type bipolar cell terminal. *J Neurophysiol* 96(4):2025–2033. doi:10.1152/jn.00364.2006

38. Frank T, Khimich D, Neef A, Moser T (2009) Mechanisms contributing to synaptic  $\text{Ca}^{2+}$  signals and their heterogeneity in hair cells. *Proc Natl Acad Sci U S A* 106(11):4483–4488. doi:[10.1073/pnas.0813213106](https://doi.org/10.1073/pnas.0813213106)
39. Jackman SL, Choi SY, Thoreson WB, Rabl K, Bartoletti TM, Kramer RH (2009) Role of the synaptic ribbon in transmitting the cone light response. *Nat Neurosci* 12(3):303–310. doi:[10.1038/nn.2267](https://doi.org/10.1038/nn.2267)
40. Lin HW, Furman AC, Kujawa SG, Liberman MC (2011) Primary neural degeneration in the guinea pig cochlea after reversible noise-induced threshold shift. *J Assoc Res Otolaryngol* 12(5):605–616. doi:[10.1007/s10162-011-0277-0](https://doi.org/10.1007/s10162-011-0277-0)
41. Shi L, Liu L, He T, Guo X, Yu Z, Yin S, Wang J (2013) Ribbon synapse plasticity in the cochleae of guinea pigs after noise-induced silent damage. *PLoS ONE* 8(12):e81566. doi:[10.1371/journal.pone.0081566](https://doi.org/10.1371/journal.pone.0081566)
42. Forge A, Schacht J (2000) Aminoglycoside antibiotics. *Audiol Neurotrol* 5(1):3–22
43. Dehne N, Rauen U, de Groot H, Lautermann J (2002) Involvement of the mitochondrial permeability transition in gentamicin ototoxicity. *Hear Res* 169(1–2):47–55
44. Hong SH, Park SK, Cho YS, Lee HS, Kim KR, Kim MG, Chung WH (2006) Gentamicin induced nitric oxide-related oxidative damages on vestibular afferents in the guinea pig. *Hear Res* 211(1–2):46–53. doi:[10.1016/j.heares.2005.08.009](https://doi.org/10.1016/j.heares.2005.08.009)
45. Liu K, Shi C, Sun Y, Xu Y, Shi L, Shi L, Wang X, Ji F, Hou Z, Yang S (2014) Dynamic distribution of ototoxic gentamicin entry into inner hair cells of mice. *Acta Otolaryngol* 134(4):345–351. doi:[10.3109/00016489.2013.875219](https://doi.org/10.3109/00016489.2013.875219)
46. Starr A, Picton TW, Sininger Y, Hood LJ, Berlin CI (1996) Auditory neuropathy. *Brain* 119(Pt 3):741–753
47. Ohashi T, Ochi K, Nishino H, Kenmochi M, Yoshida K (2005) Recovery of human compound action potential using a paired-click stimulation paradigm. *Hear Res* 203(1–2):192–200. doi:[10.1016/j.heares.2004.12.001](https://doi.org/10.1016/j.heares.2004.12.001)
48. Seal RP, Akil O, Yi E, Weber CM, Grant L, Yoo J, Clause A, Kandler K, Noebels JL, Glowatzki E, Lustig LR, Edwards RH (2008) Sensorineural deafness and seizures in mice lacking vesicular glutamate transporter 3. *Neuron* 57(2):263–275. doi:[10.1016/j.neuron.2007.11.032](https://doi.org/10.1016/j.neuron.2007.11.032)